USGS
science for a changing world

Techniques of Water-Resources Investigations
of the United States Geological Survey

Chapter C2

COMPUTER MODEL OF TWO-DIMENSIONAL SOLUTE TRANSPORT AND DISPERSION IN GROUND WATER

By L. F. Konikow and J. D. Bredehoeft

Book 7

AUTOMATED DATA PROCESSING AND COMPUTATIONS

at each node. If VPRM exceeds 0.09, it is assumed that the node represents a constant-head boundary condition and is treated as a fluid source or sink accordingly. At a constant-head node the difference in head between the aquifer and the source bed is used to determine whether the node represents a fluid source or sink (for example, lines F2500–F2520).

Subroutine CNCON

This subroutine computes the change in concentration at each node and at each particle for the given time increment. Equation 39, which denotes the change in concentration resulting from sources, divergence of velocity, and changes in saturated thickness, is solved on lines G350–G610. On the G520 the value of the storage coefficient is checked to determine whether the aquifer is confined or unconfined. It assumes that if $S<0.005$, then the aquifer is confined and $\partial b/\partial t=0$. If $S\geqq 0.005$, the model assumes that $\partial b/\partial t = \partial h/\partial t$. If this criterion is not appropriate to a particular aquifer system, then line G520 should be modified accordingly. The change in concentration caused by hydrodynamic dispersion is computed on lines G640–G770 as indicated by equations 37 and 38.

The nodal changes in concentration caused by convective transport are computed on lines G850–G940. The number of cells that are void of particles at the new time level are also counted in this set of statements on lines G880–G910, and then compared with the critical number of void cells (NZCRIT) to determine if particles should be regenerated at initial positions before the next time level is started (lines G960–G1020).

The new (time level k) concentrations at nodes are computed on the basis of the previous concentration at time $k-1$ and the change during $k-1$ to k. The adjustment at nodes is accomplished on lines G1060–G1180, while the concentration of particles is adjusted on lines G1210–G1360.

A mass balance for the solute is next computed (lines G1400–G1730) at the end of each time increment. In computing the mass of solute withdrawn or leaking out of the aquifer at fluid sinks, the concentration at the sink node is assumed to equal the nodal concentration computed at time level $k-1$.

Subroutine OUTPT

This subroutine prints the results of the flow model calculations. When invoked, the subroutine prints (1) the new hydraulic head matrix (lines H190–H260), (2) a numeric map of head values (H300–H390), and (3) a drawdown map (H510–H710). This subroutine also computes a mass balance for the flow model and estimates its accuracy (H420–H820). A mass balance is performed both for cumulative volumes since the initial time and for flow rates during the present time step. The mass balance results are printed on lines H840–H930.

Subroutine CHMOT

This subroutine prints (1) maps of concentration (lines I250–I380), (2) change in concentration from initial conditions (I440–I580), and (3) the results of the cumulative mass balance for the solute (I670–I860). The accuracy of the chemical mass balance is estimated on lines I610–I660 using equations 62 and 64. The former is not computed if there was no change in the total mass of solute stored in the aquifer. The latter is not computed if the initial concentrations were zero everywhere. Lines I890–I1140 serve to print the head and concentration data recorded at observation wells. These data are recorded after each time step for a transient flow problem and after each particle movement for a steady-state flow problem. The data are printed after every 50 time increments and at the end of the simulation period.

Evaluation of Model

Comparison with analytical solutions

The accuracy of the numerical solution to the solute-transport equation can be evalu-

ated in part by analyzing relatively simple problems for which analytical solutions are available and then comparing the numerical calculations with the analytical solution. Figure 11 presents such a comparison for a problem of one-dimensional steady-state flow through a homogeneous isotropic porous medium. The analytical solution is obtained with the following equation presented by Bear (1972, p. 627):

$$\frac{C(x,t)-C_0}{C_1-C_0}=\frac{1}{2}\text{erfc}\left\{-\frac{x-qt/\epsilon}{\sqrt{4D_Lt}}\right\} \quad (68)$$

where

erfc is the complimentary error function, and

$q=\epsilon V$ is the specific discharge, LT^{-1}.

Bear (1972, p. 627) shows that equation 68 is subject to the following initial conditions:

$$t\leq 0,\quad -\infty<x<0,\quad C=C_0$$
$$0\leq x<+\infty,\quad C=C_1$$

and to the following boundary conditions:

$$t>0,\quad x=\pm\infty,\quad \partial C/\partial x=0$$
$$x=+\infty,\quad C=C_1$$
$$x=-\infty,\quad C=C_0.$$

The general computer program presented in this report was modified in three simple ways for application to a problem equivalent to the one for which the analytical solution was derived. First, the program's arrays were redimensioned to 3 by 50 rather than 20 by 20. The aquifer (or column of porous medium) was thus represented by a 1-by-48 array of nodes. A grid spacing of 10 ft (3.05 m) was used. Second, the flow velocity was specified as a constant value, rather than being computed implicitly on the basis of hydraulic gradients and hydraulic conductivity. Third, the first (upstream) node of the aquifer was specified as a constant-concentration boundary, so that the concentration at node (2,2) was always equal to C_0 of

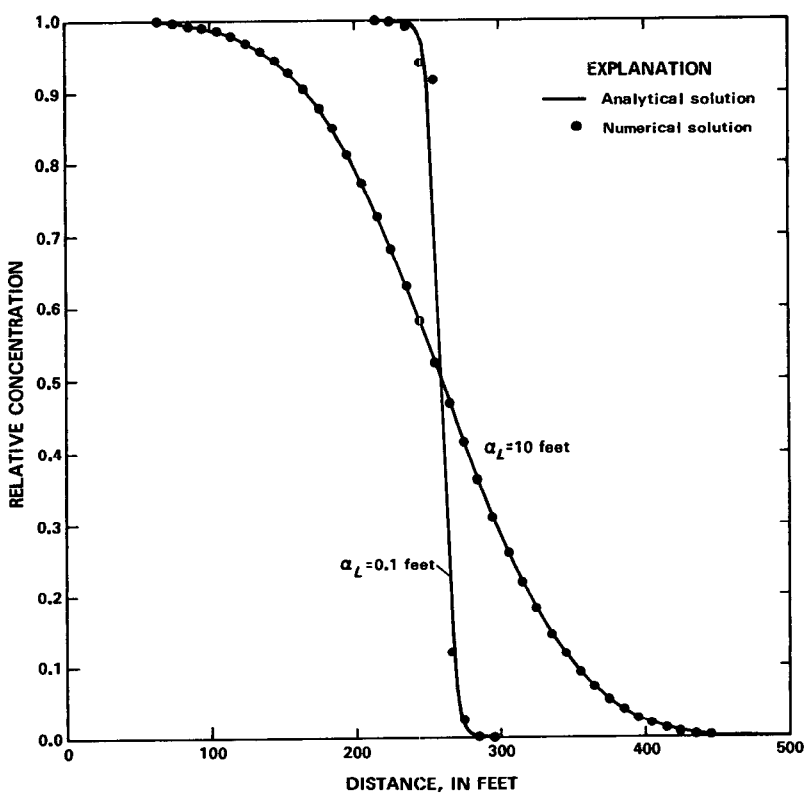

Figure 11.—Comparison between analytical and numerical solutions for dispersion in one-dimensional, steady-state flow.

equation 68. In the analysis of one-dimensional test problems, it was assumed that porosity equals 0.35, velocity equals 3.0×10^{-4} ft/s (9.1×10^{-5} m/s), and time equals 10.0 days.

As shown in figure 11, comparisons between the analytical and numerical solutions were made for two different values of dispersivity. For the higher dispersion there was essentially an exact agreement between the two curves. In the case of low dispersion, there is a very small difference at some nodes between the concentrations computed analytically and those computed numerically. This difference is caused primarily by the error in computing the concentration at a node as the arithmetic average of the concentrations of all particles located in that cell. This is not considered to be a serious problem since this error is not cumulative. Also note in the case of low dispersion that the grid spacing (10 ft or 3.05 m) was coarse relative to the width of the breakthrough curve between concentrations of 0.05 and 0.95. Nevertheless, the numerical model still accurately computed the shape and position of the front.

In computing the numerical solutions shown in figure 11 the program was executed using nine particles per cell and with CELDIS = 0.50 (γ in equations 54–55). The 10-day simulation required 52 time increments and used about 40 seconds of cpu on a Honeywell 60/68 computer.

An analytical solution is also available for the problem of plane radial flow in which a well continuously injects a tracer at constant rate q_w and constant concentration C_0. Bear (1972, p. 638) indicates that the following equation is appropriate for this problem (although there are some limitations discussed by Bear):

$$\frac{C}{C_0}=\frac{1}{2}\text{erfc}\left\{\frac{r^2/2-Gt}{\sqrt{4/3\alpha_1\bar{r}^3}}\right\} \qquad (69)$$

where

$G = \dfrac{q_w}{2\pi\epsilon b} = Vr$;

r is the radial distance from the center of the well, L; and

$\bar{r}=(2Gt)^{1/2}$ is the average radius of the body of injected water, L.

Again, the general computer program had to be somewhat modified to permit a suitable comparison to be made between the analytical solution and the numerical model. One change involved the direct calculation of velocity at any point based on its distance from the well using the following equation:

$$V=\frac{q_w}{2\pi r\epsilon b}. \qquad (70)$$

The other significant change was made in subroutine GENPT to allow the initial placement of 16 particles per cell, rather than the present maximum of 9. In the analysis of test problems for radial flow, it was assumed that porosity equals 0.35, the injection rate (q_w) equals 1.0 ft^3/s (0.028 m^3/s), saturated thickness equals 10.0 ft (3.05 m), and longitudinal dispersivity equals 10.0 ft (3.05 m).

The application of the method of characteristics, which was written for two-dimensional Cartesian coordinates, to a problem involving radially symmetric divergent flow represents a severe test of the model. Nevertheless, it can be seen in figure 12 that there is good agreement between the analytical and numerical solutions after both relatively short and long times. However, the presence of some numerical dispersion is evident, particularly for the longer time. The numerical dispersion is introduced in part during the regeneration of particles after the number of cells void of particles has exceeded the critical number. The geometry of initial particle placement minimized this problem in cells that lay in the same row or column of the grid as the injection well. The circles in figure 12, which indicate concentration values computed at these nodes, agree closely with the analytical solution. The greatest errors occur at nodes on radii from the injection well that are neither parallel to nor 45° from the main axes of the grid. These results indicate that this Cartesian coordinate model is not best suited for application to purely radial flow problems. However, if radially divergent flow is limited to areas of several

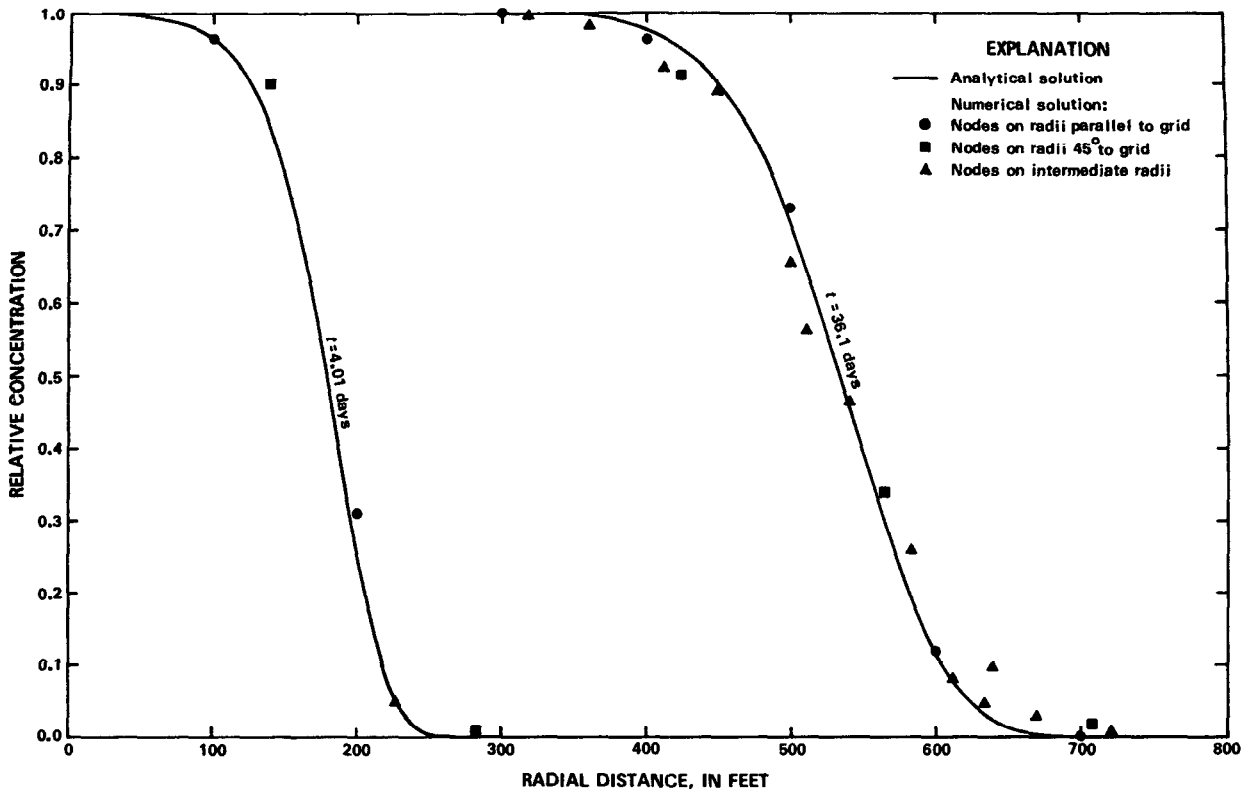

Figure 12.—Comparison between analytical and numerical solutions for dispersion in plane radial steady-state flow.

rows and columns within a more uniform regional flow field, the model will accurately compute concentration distributions. To apply the method of characteristics to a problem of plane radial flow, it would be best to rewrite the program in a system of radial coordinates, which should improve the accuracy for those problems to the same order shown in figure 11 for the analysis of one-dimensional flow.

Mass balance tests

The accuracy and precision of the numerical solution can also be partly evaluated by computing the magnitude of the error in the mass balance. The mass balance error will depend on the nature of the problem and will vary from one time step to the next. During the development of the program, the model was applied to a variety of hypothetical solute-transport problems to assure its flexibility, transferability, and accuracy under a wide range of conditions. To illustrate the range in mass balance errors that might be expected and some of the factors that affect it, several of these problems are presented here.

Test problem 1—spreading of a tracer slug

The first test described here was designed to evaluate the accuracy of simulating the processes of convective transport and dispersion independent of the effects of chemical sources. Thus, a slug of tracer was initially placed in four cells of a grid whose boundary conditions generated a steady-state flow field that was moderately divergent in some places and moderately convergent in other places, as illustrated in figure 13. The aquifer was assumed to be homogeneous and isotropic. Because flow was assumed to be in steady state, the storage coefficient was set equal to 0.0. The parameters used to define problem

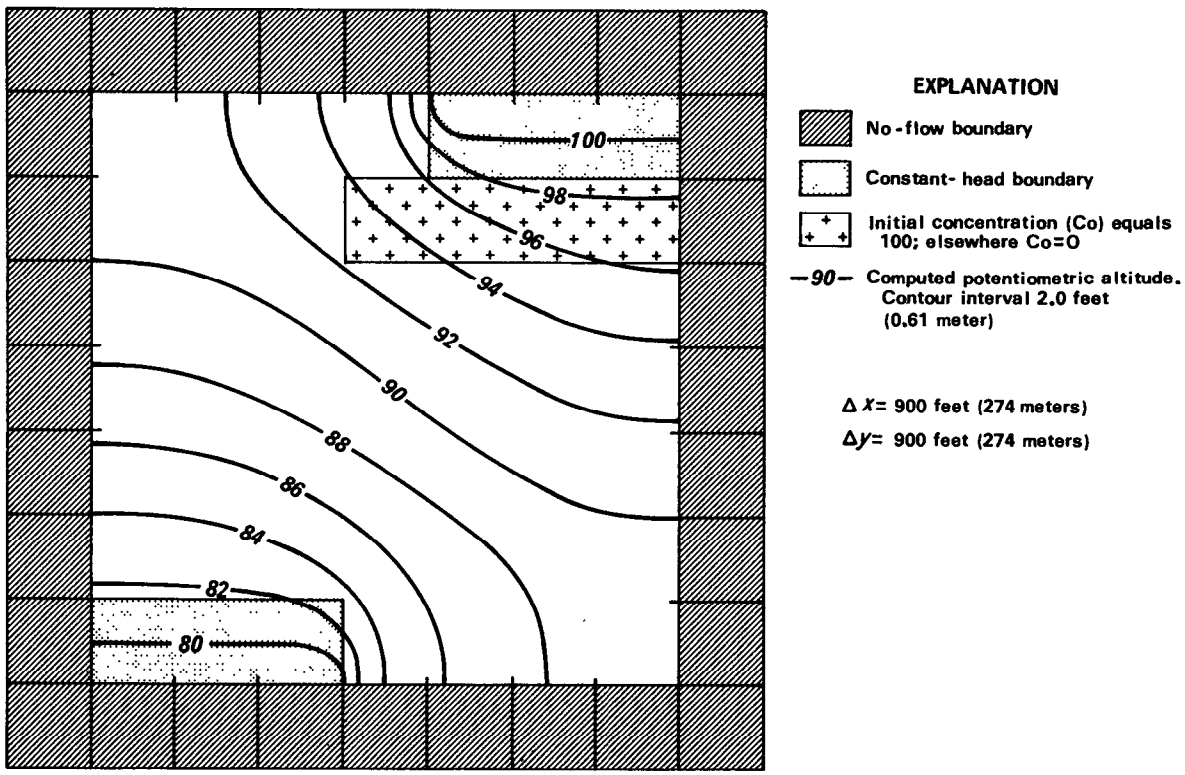

Figure 13.—Grid, boundary conditions, and flow field for test problem 1.

1 are listed in table 2. The slug of known mass was then allowed to spread downgradient for a period of 2.0 years.

Table 2.—Model parameters for test problem 1

Aquifer properties	Numerical parameters
K=0.005 ft/s (1.5×10^{-3} m/s)	Δx=900 ft (274 m)
b=20.0 ft (6.1 m)	Δy=900 ft (274 m)
S=0.0	CELDIS=0.49
ε=0.30	NPTPND=9
α_T/α_L=0.30	

The model first computed a steady-state head distribution, shown in figure 13, and velocity field. The model required 12 time increments (or particle movements) to simulate a 2.0-year period. The model was run to simulate conditions of no dispersion (α_L=0.0 ft) as well as moderate dispersion (α_L=100 ft or 30.5 m). The mass balance error computed using equation 64 is shown in figure 14 for both conditions. In these tests the error averages 1.9 percent and is always within a range of ±8 percent. Much of the error is related to the calculation of nodal concentrations based on the arithmetic mean of particle concentrations in each cell. When a particle moves across a cell boundary, its area of influence shifts entirely from the first node to the second. Thus, depending on the local density of points and local concentration gradients, the use of an arithmetic mean to compute nodal concentrations may give too much weight to some particles and too little weight to others. The use of a weighted mean, in which the weighting factor is a function of the distance between a node and a particle, reduced the error to some degree. But the improvement in precision was small compared with the increase in computational requirements, so this algorithm was not included in the general program. Because the error caused by using an arithmetic mean is not cumulative, it is not considered a serious

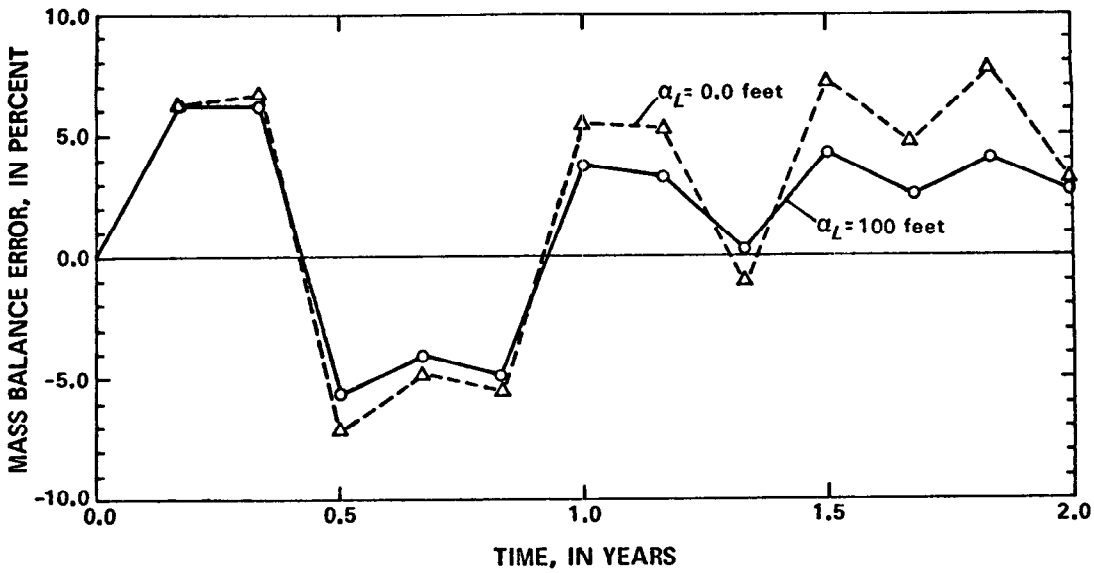

Figure 14.—Mass balance errors for test problem 1.

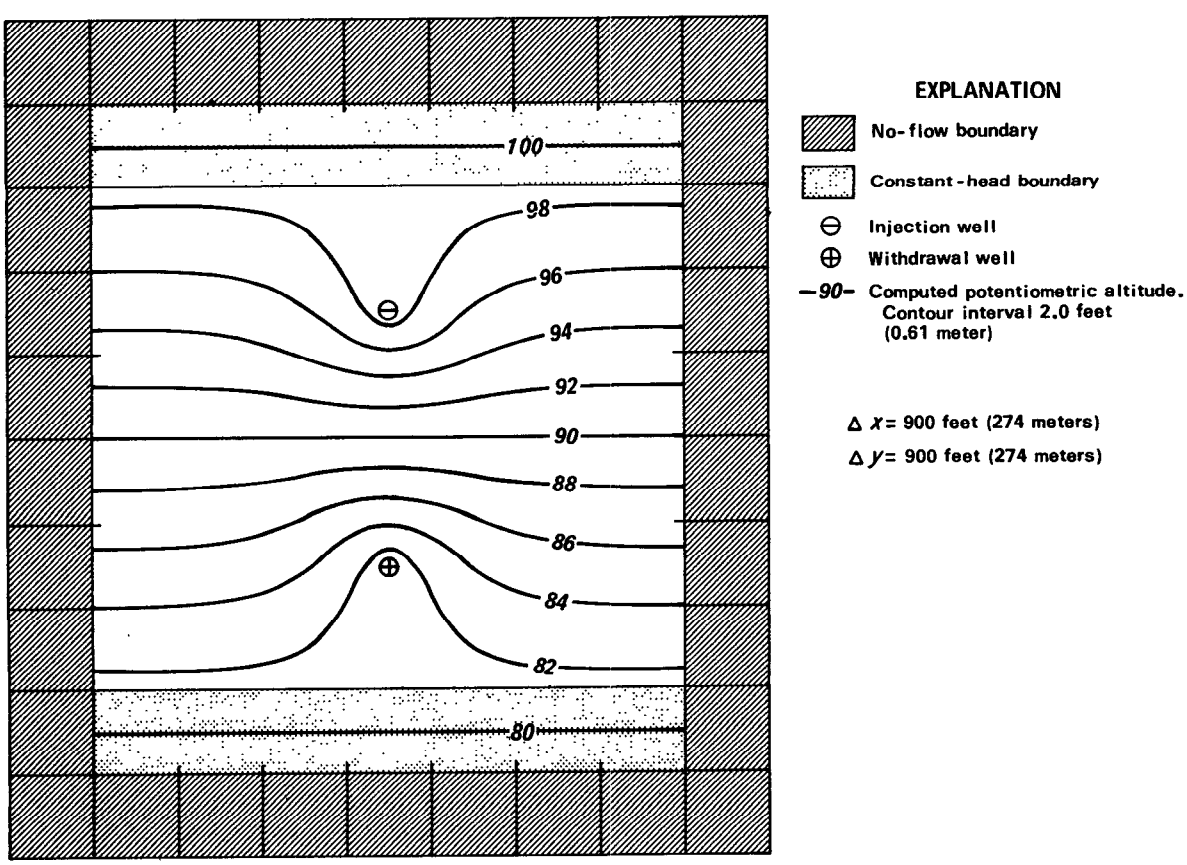

Figure 15.—Grid, boundary conditions, and flow field for test problem 2.

problem. Furthermore, figure 14 shows that the error decreases for a higher dispersivity because dispersion smooths out sharp fronts and minimizes strong concentration gradients.

Test problem 2—effects of wells

The second problem was designed to evaluate the application of the model to problems in which the flow field is strongly influenced by wells. The grid and boundary conditions used to define this problem are illustrated in figure 15. The problem consists of one injection well and one withdrawal well, whose effects are superimposed on a regional flow field controlled by two constant-head boundaries. The parameters for problem 2 are defined in table 3. The aquifer was also assumed to be homogeneous and isotropic. The model simulated a period of 2.4 years and assumed steady-state flow.

The model required 18 time increments (or particle movements) to simulate a 2.4-year period of solute transport. Problem 2 was also evaluated for conditions of no dispersion ($\alpha_L = 0.0$ ft) as well as moderate dispersion ($\alpha_L = 100$ ft or 30.5 m). The mass balance error was computed using equation 62 and is shown in figure 16 for both conditions. The average of the 36 values shown in figure 16 is -0.06 percent; the error always falls within the range of ± 8 percent. It can be seen that in this case the errors are essentially coincident for almost 1 year, after which the error appears to be dependent on the magnitude of dispersion. However, the model output showed that when $\alpha_L = 100$ ft (30.5 m), the leading edge of the breakthrough curve (or chemical front) reaches the constant-head sink just prior to 1.0 year. When $\alpha_L = 0.0$ ft, the leading edge of the breakthrough curve still had not entered the constant-head sink after 2.4 years. Because the two curves in figure 16 are essentially coincident prior to 1.0 year, it thus appears that the divergence of the two curves is not caused directly by the difference in dispersivity. Rather, it is related to the difference in arrival times at the hydraulic sinks and is a direct effect of the manner in which con-

Table 3.—Model parameters for test problems 2 and 3

Aquifer properties and stresses	Numerical parameters
$K = 0.005$ ft/s (1.5×10^{-3} m/s)	$\Delta x = 900$ ft (274 m)
$b = 20.0$ ft (6.1 m)	$\Delta y = 900$ ft (274 m)
$S = 0.0$	CELDIS = 0.50
$\epsilon = 0.30$	NPTPND = 9
$\alpha_T/\alpha_L = 0.30$	
$C' = 100.0$	
$C_0 = 0.0$	
$q_w = 1.0$ ft^3/s (0.028 m^3/s)	

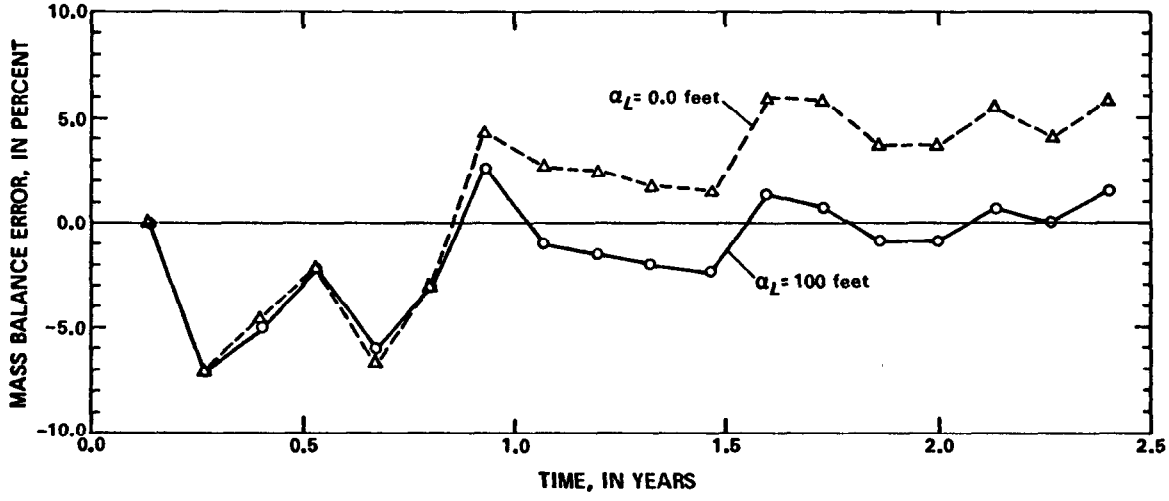

Figure 16.—Mass balance errors for test problem 2.

centrations are computed at sink nodes and (or) the method of estimating the mass of solute removed from the aquifer at sink nodes during each time increment.

Test problem 3—effects of user options

In addition to the input options that control the form or frequency of the output, there are two execution parameters that must be specified by the user and influence the accuracy, precision, and efficiency (or computational cost) of the solution to a particular problem. These execution parameters are the initial number of particles per node (NPTPND) and the maximum fraction of the grid dimensions that particles are allowed to move (γ in equations 54–55 or CELDIS in the program). The third test problem was designed to allow an evaluation of both of these parameters. As illustrated in figure 17, this problem consists of one withdrawal well located in a regional flow field that is controlled by two constant-head boundaries. The contamination sources are three central nodes along the upgradient constant-head boundary. The model parameters for test problem 3 are the same as for test problem 2, as listed in table 3. However, for test problem 3 solutions were obtained using a range in values for CELDIS and NPTPND.

The solution to this problem was found to be sensitive to the density of tracer particles used in the simulation. Figure 18 shows how the error in the mass balance varied with time for cases of NPTPND equal to 4, 5, 8, and 9. Table 4 lists the execution time and the mean and standard deviation of the mass balance error for each case. These data clearly indicate that the accuracy and precision

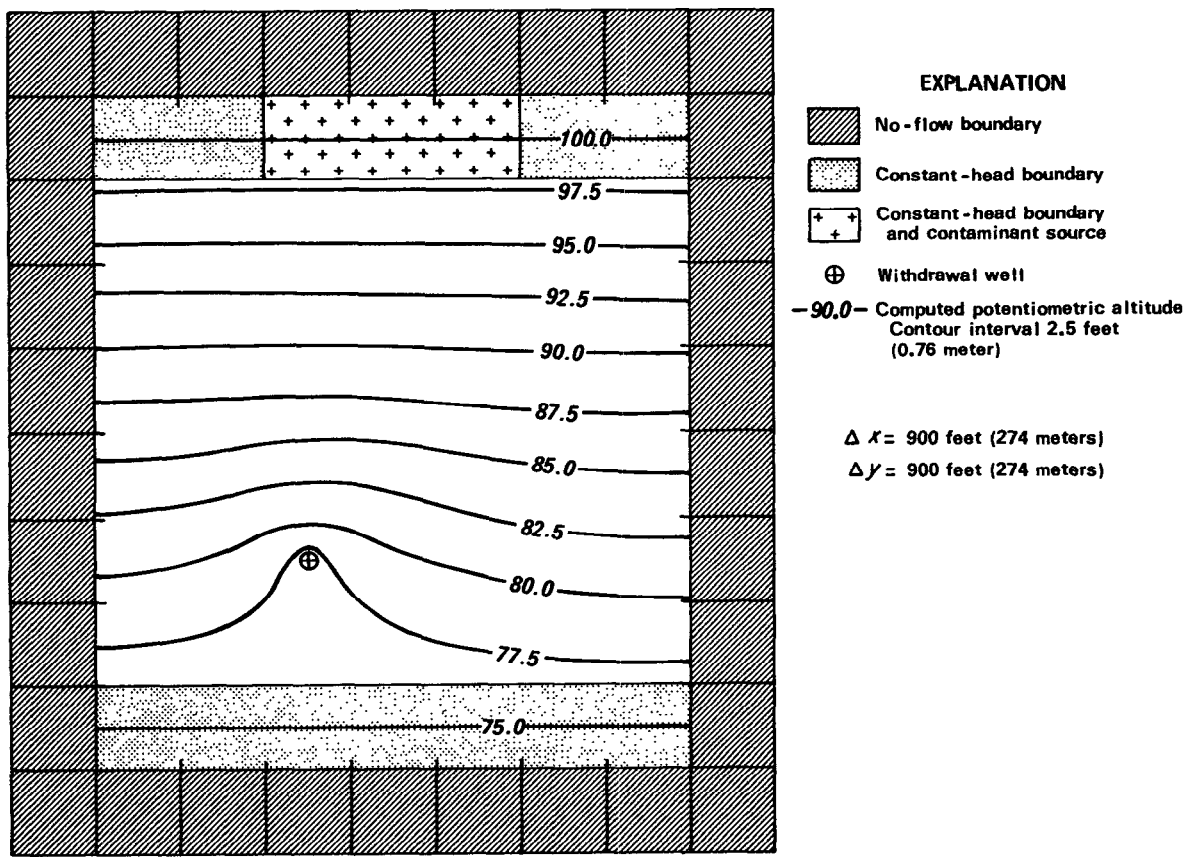

Figure 17.—Grid, boundary conditions, and flow field for test problem 3.

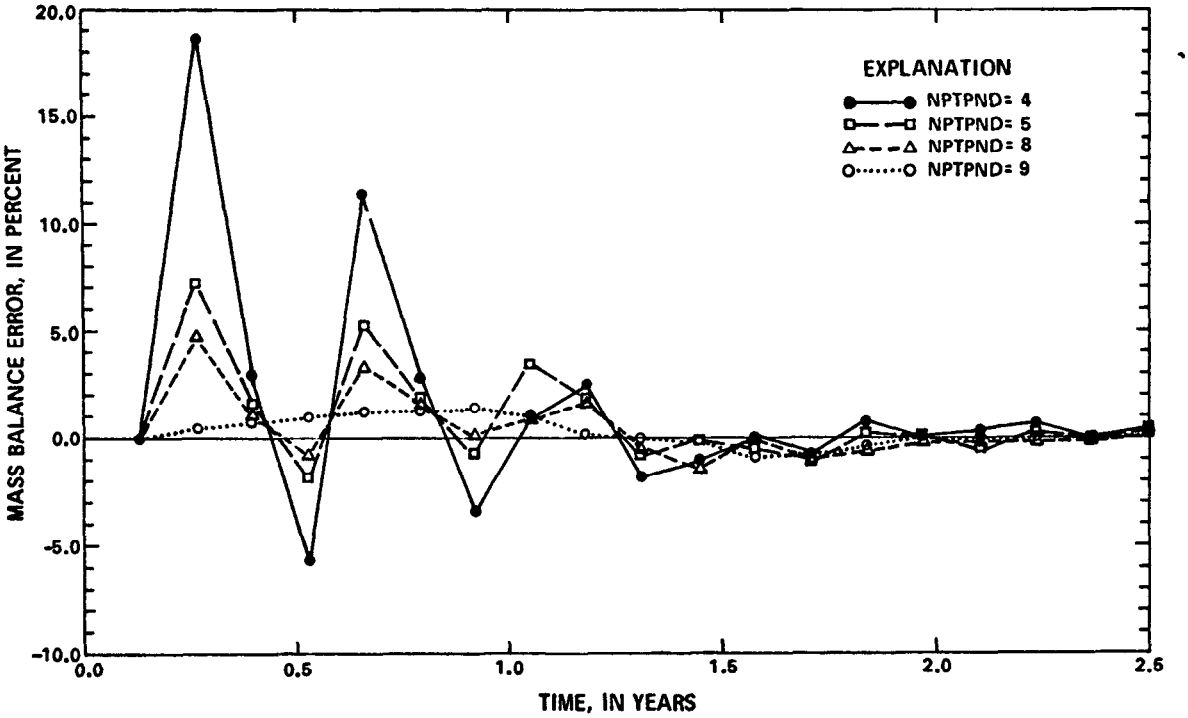

Figure 18.—Effect of NPTPND on mass balance error for test problem 3; CELDIS=0.50 in all cases.

Table 4.—Effect of NPTPND on accuracy, precision, and efficiency of solution to test problem 3

NPTPND	cpu-seconds [1]	Mass balance error (percent) Mean	Mass balance error (percent) Standard deviation
4	12.8	1.49	5.33
5	14.0	.90	2.29
8	17.9	.48	1.53
9	19.2	.26	.69

[1] The program was executed on a Honeywell 60/68 computer; CELDIS=0.50.

of the solution are directly proportional to particle density, while the efficiency of the solution is inversely related to NPTPND. In other words, a better solution will cost more. It is important to note that the oscillations or scatter shown in figure 18 decrease with time and that there is essentially no difference among the solutions and among the mass balance errors for times greater than about 1.5 years.

Next the effect of CELDIS (or γ) was evaluated for test problem 3 by setting NPTPND=9 and running the model with several possible values of CELDIS. Figure 19 shows how the error in the mass balance varied with time for cases of CELDIS equal to 0.25, 0.50, 0.75, and 1.00. Table 5 lists the

Table 5.—Effect of CELDIS on accuracy, precision, and efficiency of solution to test problem 3

CELDIS	cpu-seconds [1]	Mass balance error (percent) Mean	Mass balance error (percent) Standard deviation
0.25	34.6	1.50	2.99
.50	19.2	.26	.69
.75	14.4	.56	.69
1.00	12.1	.25	1.48

[1] The program was executed on a Honeywell 60/68 computer; NPTPND=9.

execution time and the mean and standard deviation of the mass balance error for each case. These data indicate that the relationship between CELDIS and the mass balance error is not as simple and straightforward as for NPTPND. It is apparent that the results for 0.50, 0.75, and 1.00 are similar, and of these, the results for CELDIS=0.50 ap-

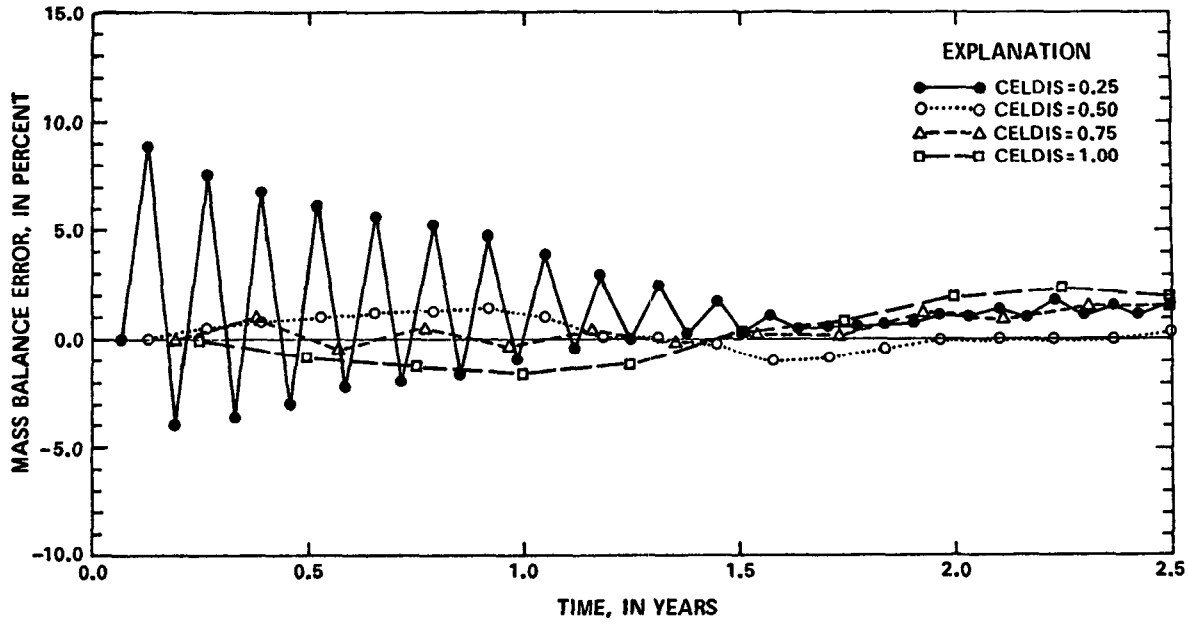

Figure 19.—Effect of CELDIS on mass balance error for test problem 3; NPTPND=9 in all cases.

pear to be the best. However, when CELDIS was reduced to 0.25, the error oscillated strongly for about 1.5 years before apparently converging to a small error within the range of the other curves. This oscillation occurred because the maximum distance a particle could move (25 percent of the grid dimensions) was less than the spacing between particles (33 percent of the grid dimensions for NPTPND=9). Thus, convective transport across the boundaries of cells could not be adequately represented for any single time step in those parts of the grid where the concentration was changing significantly with time. But over two successive time increments the error would average out to a minimum. As the contaminated area increases in size over time, the error in computed concentrations at cells near the front (that is, in areas of steep concentration gradient) becomes an increasingly smaller percentage of the total mass of solute present in the aquifer. Hence, the mass balance error generally tends to approach a minimal range with time for these types of problems.

The effects of NPTPND and CELDIS on the mass balance error are problem dependent. In problems for which CELDIS is not the limiting stability criterion, varying CELDIS will have no effect on the solution. Because of the possible tradeoff between accuracy and efficiency, it is recommended in general that the model user specify NPTPND as 4 or 5 and CELDIS as 0.75 to 1.0 for runs made during the early stages of model calibration when frequent runs are made and maximum efficiency is desired. For final runs when maximum accuracy is desired, set NPTPND equal to 9 and CELDIS equal to 0.50.

Possible program modifications

The program presented here represents a basic and general solute-transport model. Some program modifications may be desirable or even necessary to allow the model to be applied efficiently to a particular field problem. Some changes might require only minor adjustments, while others might involve major rewriting of the program. The purpose of this section is to discuss some of the modifications that might commonly be considered, and that might be incorporated into the present basic model, rather than using an entirely different solution technique.

Coordinate system and boundary conditions

After the finite-difference grid is designed, the first program modification that should be made is to modify the array dimensions for the specific grid used. This will permit the most efficient use of computer storage. The array sizes should be set equal to NX, NY, and NPMAX, which are specified on Input Card 2. The maximum number of particles, NPMAX, may be computed from the following equation:

$$NPMAX \cong (NX-2)(NY-2)(NPTPND) + (N_s)(NPTPND) + 250 \quad (71)$$

where

N_s is the number of nodes that represent fluid sources, either at wells or at constant-head cells.

The values of NX and NY should be substituted for the 20-by-20 arrays contained in COMMON statements PRMK, HEDA, HEDB, CHMA, CHMC, and DIFUS, and in DIMENSION statements on lines C170, G200, H140, and I160. The value of NPMAX should replace 3200 in the PART array in all the CHMA COMMON statements.

Although this program is designed for application to two-dimensional areal flow problems, it can be applied directly to two-dimensional cross sections. In this case the z-coordinate would replace the y-coordinate. Then the user would have to assume and specify unit width (THCK array) for Δy and substitute hydraulic conductivity for transmissivity in data set 3 of attachment III. If the problem involves transient flow, then specific storage (S_s) should be substituted for the storage coefficient. Also, if recharge or discharge is to be specified through the RECH array (data set 5), values should be divided by the thickness of the layer (Δz) to reduce the dimensionality of the stress rate to (T^{-1}) rather than (LT^{-1}) as indicated in the documentation. In applying the cross-sectional model to a field problem it is important that conditions meet the inherent assumption that there exist no significant components of flow into or out of the plane of the section. Because this assumption would probably be impossible to meet in the vicinity of a pumping well, the use of the REC array (data set 2) should usually be limited to representing special or known-flux boundary conditions.

The program can also be applied directly and simply to one-dimensional problems. In this case one of the dimensions (NX or NY) should be reduced to a value of 3, of which the outer two are used to represent the no-flow boundaries around the one-dimensional row or column.

The most complex type of change would involve rewriting the program for application to other than a two-dimensional rectangular grid. One possibility includes problems of flow to or from wells in which radial symmetry can be assumed. This would allow variables to be expressed in terms of r-z coordinates. Another possibility is to simulate three-dimensional flow in x-y-z coordinates. A three-dimensional finite-difference flow model is available (Trescott, 1975) and would be compatible with the method-of-characteristics solution to the solute-transport equation.

It is sometimes convenient to separately associate certain parts of the grid or certain boundary conditions with corresponding field conditions or hydrologic units. The analysis of flow patterns and water-quality changes may then be aided by performing separate mass balances (or budgets) for each characteristic type of node. The nodal types or zones can be conveniently identified through the NODEID array. Then the mass balance routines in subroutines CNCON and (or) OUTPT would have to be modified to tally fluxes separately for each NODEID; for an example, see Konikow (1977). Similarly, if a coupled stream-aquifer system is being considered, a separate subroutine may be added to route streamflow downstream and progressively account for ground-water gains and losses and for tributary inflow or diversions. An example of such a modification is discussed by Konikow and Bredehoeft (1974).

For certain types of problems it may be desirable to be able to specify a constant-concentration boundary condition. The pro-

gram could be modified to allow this by using a predetermined value or range in values of NODEID to identify this type of boundary. Then a statement could be added between lines G1090 and G1100 to reset the concentration at the node equal to the constant concentration where this condition is specified. The value of the constant concentration can be stored in the CNRECH array. Note that the mass balance calculation as presently written will not account for the mass of solute added or removed at a constant-concentration boundary.

Basic equations

The basic equations that are solved by this model were derived under a number of limiting assumptions. Some of these assumptions can be overcome through modifications of the basic equations and corresponding changes in the program.

The program assumes that molecular diffusion is negligible. But if it is necessary to consider the process of molecular diffusion in a particular problem, the coefficient of hydrodynamic dispersion (D_{ij}) can be redefined as the sum of the coefficient of mechanical dispersion, which is defined by the right side of equation 5, and a coefficient of molecular diffusion. The consequent program modification would have to be made only in subroutine VELO (lines E1280–E1680).

The solute-transport equation can also be modified to include the effects of first-order chemical reactions, as was done by Robertson (1974). The reaction term could be included in the right side of equation 39. The corresponding program modification would be required in subroutine CNCON.

In certain problems the range in concentrations may be so great that the dependence of fluid properties, such as density and viscosity, on the concentration may have to be considered because of the dependence of fluid flow on variations in fluid properties. In this case the flow equation (eq 1) would have to be rewritten in terms of fluid pressure, rather than hydraulic head, such as equation 15 of Bredehoeft and Pinder (1973, p. 197). Then the program can be modified to iterate between the solutions to the flow and solute-transport equations if the change in fluid properties at any node exceeds some criterion during one time increment.

The flow equation can also be modified for application to unconfined aquifers in which the saturated thickness is a direct function of water-table elevation. This would require the inclusion of steps in subroutine ITERAT to correct the transmissivity for changes in saturated thickness. Such a feature is included in the two-dimensional flow model documented by Trescott, Pinder, and Larson (1976).

Input and output

The input and output formats have been designed for flexibility of use and general compatibility with the analysis of a variety of types of flow problems. If any of the formats are not suitable for use with a particular problem, they should be modified accordingly. All input formats are described in attachment III and contained in subroutine PARLOD in the program.

It has been assumed that several aquifer parameters are constant and uniform in space, such as storage coefficient, effective porosity, and dispersivity. If any of these are known to vary in space, they should be redefined as two-dimensional arrays. Then statements to allow these arrays to be read into the program should be added to subroutine PARLOD. Similarly, values of leakance and source concentrations (CNRECH) are only read in data set 7, where values can be associated only with a limited number of unique node identification codes. If the variations of these parameters are known on a more detailed scale, then they too can be read as additional data sets by adding appropriate statements to subroutine PARLOD. For example, a typical sequence of statements for reading one data set is represented by lines B2650–B2750, where the initial water-table elevations (data set 8) are read. This sequence of statements can then be replicated for reading in a different data set and inserted into subroutine PARLOD.

A labeled listing of the input data deck for test problem 3 is provided in attachment IV. This example illustrates the use of the data input formats specified in attachment III and shows that only a few data cards are required by the model to simulate a relatively simple problem. This example will also allow the user to verify that his program deck and computer yield essentially the same results as obtained by the documented program. Thus, selected parts of the output for test problem 3 are included in attachment V. Not all of the printed output from test problem 3 has been duplicated in attachment III. Instead, it contains only a sufficient selection to illustrate the type and form of output provided by the model, as well as to allow the user to compare his calculated values of critical parameters, such as head, velocity, and concentration, with the values computed by the documented model.

Conclusions

The model presented in this report can simulate the two-dimensional transport and dispersion of a nonreactive solute in either steady-state or transient ground-water flow. The program is general and flexible in that it can be readily and directly applied to a wide range of types of problems, as defined by aquifer properties, boundary conditions, and stresses. However, some program modifications may be required for application to specialized problems or conditions not included in the general model.

The accuracy of the numerical results can be evaluated by comparison with analytical solutions only for relatively simple and idealized problems; in these cases there was good agreement between the numerical and analytical results. Mass balance tests also help to evaluate the accuracy and precision of the model results. The error in the mass balance is generally less than 10 percent. The range in mass balance errors is commonly the greatest during the first few time increments, but tends to decrease and stabilize with time. For some problems the accuracy and precision of the numerical results may be sensitive to the initial number of particles placed in each cell and to the size of the time increments, as determined by the stability criteria for the solute-transport equation. The results of several numerical experiments suggest that the accuracy and precision of the results are essentially independent of the magnitude of the dispersion coefficient, and comparable accuracies are attained for high, low, or zero dispersivities.

References Cited

Aris, Rutherford, 1962, Vectors, tensors, and the basic equations of fluid mechanics: Englewood Cliffs, N. J., Prentice-Hall, 286 p.

Bear, Jacob, 1972, Dynamics of fluids in porous media: New York, Am. Elsevier Publishing Co., 764 p.

Bredehoeft, J. D., and Pinder, G. F., 1973, Mass transport in flowing groundwater: Water Resources Research, v. 9, no. 1, p. 194–210.

Garder, A. O., Peaceman, D. W., and Pozzi, A. L., Jr., 1964, Numerical calculation of multidimensional miscible displacement by the method of characteristics: Soc. Petroleum Engineers Jour., v. 4, no. 1, p. 26–36.

Konikow, L. F., 1977, Modeling chloride movement in the alluvial aquifer at the Rocky Mountain Arsenal, Colorado: U.S. Geol. Survey Water-Supply Paper 2044, 43 p.

Konikow, L. F., and Bredehoeft, J. D., 1974, Modeling flow and chemical quality changes in an irrigated stream-aquifer system: Water Resources Research, v. 10, no. 3, p. 546–562.

Konikow, L. F., and Grove, D. B., 1977, Derivation of equations describing solute transport in ground water: U.S. Geol. Survey Water-Resources Investigatons 77–19, 30 p.

Lohman, S. W., 1972, Ground-water hydraulics: U.S. Geol. Survey Prof. Paper 708, 70 p.

Pinder, G. F., and Bredehoeft, J. D., 1968, Application of the digital computer for aquifer evaluation: Water Resources Research, v. 4, no. 5, p. 1069–1093.

Pinder, G. F., and Cooper, H. H., Jr., 1970, A numerical technique for calculating the transient position of the saltwater front: Water Resources Research, v. 6, no. 3, p. 875–882.

Prickett, T. A., and Lonnquist, C. G., 1971, Selected digital computer techniques for groundwater resource evaluation: Illinois Water Survey Bull. 55, 62 p.

Reddell, D. L., and Sunada, D. K., 1970, Numerical simulation of dispersion in groundwater aquifers: Colorado State Univ. Hydrology Paper 41, 79 p.

Robertson, J. B., 1974, Digital modeling of radioactive and chemical waste transport in the Snake River Plain aquifer at the National Reactor Testing Station, Idaho: U.S. Geol. Survey Open-File Rept. IDO–22054, 41 p.

Robson, S. G., 1974, Feasibility of digital water-quality modeling illustrated by application at Barstow, California: U.S. Geol. Survey Water-Resources Investigations 46–73, 66 p.

Scheidegger, A. E., 1961, General theory of dispersion in porous media: Jour. Geophys. Research, v. 66, no. 10, p. 3273–3278.

Trescott, P. C., 1975, Documentation of finite-difference model for simulation of three-dimensional ground-water flow: U.S. Geol. Survey Open-File Rept. 75–438, 32 p.

Trescott, P. C., Pinder, G. F., and Larson, S. P., 1976, Finite-difference model for aquifer simulation in two dimensions with results of numerical experiments: U.S. Geol. Survey Techniques of Water-Resources Investigations, Book 7, Chap. C1, 116 p.

von Rosenberg, D. U., 1969, Methods for the numerical solution of partial differential equations: New York, Am. Elsevier Publishing Co., 128 p.

COMPUTER PROGRAM AND RELATED DATA